JOURNAL OF SOLID STATE CHEMISTRY **29**, 355–365 (1979)

In Situ Mössbauer Spectroscopy Studies of the Electrochemical Reaction of Lithium with $KFeS_2$

A. J. JACOBSON AND L. E. McCANDLISH

Exxon Research and Engineering Company, P.O. Box 45, Linden, New Jersey 07036

Received November 3, 1978

In situ Mössbauer spectroscopy has been used to study the electrochemical reaction of lithium with $KFeS_2$. Compositions KLi_xFeS_2 with $\Delta x = 0.25$ were obtained by coulometric titration for one complete discharge and recharge. Mössbauer spectra were obtained at each composition. Three new iron sites are identified in addition to Fe^{3+} in $KFeS_2$. A mechanism to account for the electrochemical and Mössbauer data is proposed. The end product $KLiFeS_2$ has been synthesized and found to be body-centered tetragonal with $a = 3.938(2)$ Å and $c = 13.135(5)$ Å.

Introduction

Reactions of lithium with iron compounds at ambient temperature are of considerable interest for battery applications. Electrochemical data in nonaqueous lithium cells have recently been reported for several systems including $KFeS_2$ (*1*), FeOCl (*2, 3*), FeS_2 (*3, 4*), $FePS_3$ (*5, 6*), and $V_xFe_{1-x}S_2$ ($x \leq 0.5$) (*7*). In general, the reactions of lithium with these cathode materials are more complex than those observed for transition metal dichalcogenide systems, such as TiS_2 (*8*) and much less is known concerning the reaction products formed during cell discharge and recharge.

Mössbauer spectroscopy of the ^{57}Fe nucleus is a useful technique for studying such cell reactions (*7*). The isomer shift, quadrupole splitting, and nuclear magnetic dipole splitting give information concerning the iron oxidation states and their site symmetries and are thus sensitive to the chemical and structural changes which occur during reaction. In addition the characteristic 14.4 keV γ-rays of ^{57}Fe are sufficiently energetic to penetrate reasonable thicknesses of the materials normally used in the construction of ambient-temperature experimental cells. Consequently, it is possible to examine the changes occurring at the cathode in an actual working cell. Such measurements are convenient and can provide kinetic information not obtainable in any other way. Most other spectroscopic techniques cannot be used *in situ* and diffraction methods are difficult. *In situ* X-ray diffraction measurements have been used successfully to study the electrochemical reaction of lithium with TiS_2 (*8*). In this paper the results of an *in situ* Mössbauer spectroscopic study of the electrochemical reaction of lithium with $KFeS_2$ are described. Electrochemical results and some structural data for this system were recently (*1*) reported and are summarized below.

$KFeS_2$ has a structure which comprises infinite chains of edge-shared $Fe(III)S_4$ tetrahedra (Fig. 1). K^+ ions occupy some interchain sites but vacant sites are available

0022-4596/79/090355-11$02.00/0

Printed in Great Britain

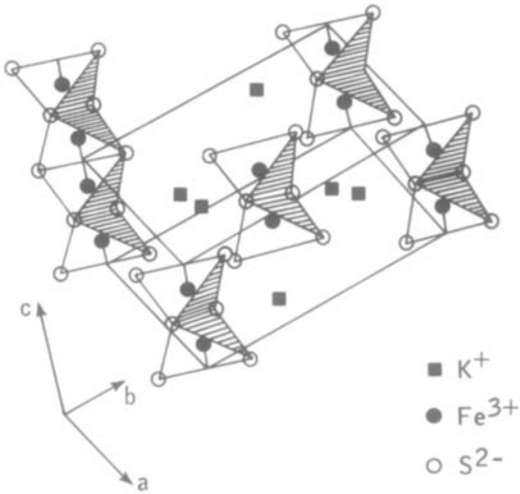

FIG. 1. Structure of $KFeS_2$.

for lithium incorporation with corresponding reduction of Fe(III) to Fe(II). Electrochemically, $KFeS_2$ can react with one lithium per $KFeS_2$. The data show, however, that the reaction is not a simple intercalation reaction but involves the conversion of $KFeS_2$ to a structurally different phase: $KLiFeS_2$. Preliminary X-ray data on samples of $KLiFeS_2$ prepared by the *n*-butyl lithium technique indicate that the new phase is tetragonal and probably belongs to the CuTe structure type. On electrochemical recharge, between 0.6 to 0.7 lithium per $KLiFeS_2$ can be easily removed but complete reformation of $KFeS_2$ can only be achieved at very low rates.

On cycling a cell under constant current conditions ($0.5\ mA/cm^2$), $KFeS_2$ is not reformed to any extent and the cell maintains good reversibility for many cycles with capacities of 0.6 to 0.7 lithium/$KFeS_2$. These data suggest that the tetragonal $KLiFeS_2$ phase behaves as a solid-solution electrode for the composition range $(0.3–0.4) \leq x \leq 1.0$ and that some lithium is required to stabilize the tetragonal structure relative to that of $KFeS_2$. To support these conclusions and to obtain more detailed structural information, Mössbauer spectra were obtained for compositions KLi_xFeS_2 over one complete discharge and recharge cycle.

Experimental

Sample Preparation and Characterization

$KFeS_2$ was prepared as large crystals by the method described in (*9*). For electrochemical studies and reactions with *n*-butyl lithium the crystallite size was reduced by grinding in a McCrone micronizing mill. Reactions with *n*-butyl lithium were performed in a helium-filled glove box using a 2.0 *M* solution of the reagent in hexane. Reactions were carried out at 25°C for 1–3 days. Excess *n*-butyl lithium was determined by reaction with a known excess of acid followed by back titration with alkali. Compositions were checked by elemental analysis. X-Ray diffraction patterns were recorded using a Philips diffractometer with samples protected from hydrolysis and oxidation by Kapton films.

Mössbauer Spectroscopy

Mössbauer spectra were recorded in transmission geometry using an Austin Science Associates linear motor and spectrometer drive operated in the constant acceleration, flyback mode. Velocity control and calibration were achieved using laser interferometry. The γ-ray source (New England Nuclear, NER-072) consisted of 9 mCi of ^{57}Co electroplated onto a 6-mm-diameter active area of 6 μm-thick palladium foil. The γ-rays were detected with a proportional counter (LND, Inc.) and the 14.4-keV signal was selected with a single-channel pulse height analyzer (Canberra). The γ-ray spectra were recorded in alternate channels of a 512-channel multichannel analyzer (Nuclear Data) operated in the multiscaling mode and synchronized with the velocity modulation of the source. The remaining analyzer channels were used to store velocity information from the interferometer and from a crystal oscillator. Mössbauer spectra were obtained from the cathode of a $KFeS_2$/Li cell constructed as described below.

Electrochemistry

A cathode was prepared by hot pressing $KFeS_2$ mixed with 10 wt% Teflon at 300°C into an expanded nickel mesh. The resulting grid had nearly 2 cm^2 of active cathode material. A bag cell was prepared by surrounding the cathode with polypropylene spacers followed by a pure lithium metal sheet as the anode. This assembly was immersed into a polypropylene bag containing a 1.5 *M* solution of electrolyte. For the Mössbauer experiment a holder was designed to accommodate this bag cell. The holder comprised two Teflon plates with circular holes, into which 1.5-in.-diameter by 0.01-in.-thick beryllium windows were sealed using epoxy adhesive for treated Teflon (Chemplast Ltd.). Into one plate a circular recess was machined above the beryllium window to accommodate two alligator clips which were used to make electrical contacts with the cell. The alligator clips were fastened by gold wires to two metal machine screws which were sealed through the plate. The two halves of the holder, separated by a butyl rubber gasket, were assembled with the active area of the cathode centered in the beryllium windows. The thickness of the gasket was such that the bag cell was firmly pressed between the holder halves when the machine screws which fastened the assembly together were tightened. All cell assembly was carried out in a helium-filled glove box and the open-circuit voltage checked before the cell was transferred to the spectrometer.

After recording the initial spectrum of the cathode, the cell was connected to a Princeton Applied Research PAR 173 potentiostat. A coulometric titration was carried out at intervals of $\Delta x = 0.25$ Li in Li_x $KFeS_2$ for one complete discharge ($x = 1.0$) and one complete recharge. Points on the discharge curve were obtained galvanostatically at current densities ranging from 0.25 mA/cm^2 at the beginning to 0.05 mA/cm^2 at the end. Low currents were necessary to obtain a complete cycle for Li_xKFeS_2 between $0 \leq x \leq 1.0$ when no graphite was added as a conducting diluent (*1*). The recharge points were obtained at constant potential (2.60 V).

After each increment in composition, the cell was rested on open circuit for 16 hr except for two points where the equilibration time was ~70 hr. The open-circuit voltage was measured after each equilibration period. Mössbauer spectra were recorded both during and after each equilibration period. A comparison of the open-circuit voltages with previous data showed that the Mössbauer cell behaved similarly to cells tested in a glove box (*1*).

Results

Mössbauer Data

The Mössbauer spectra are displayed in Fig. 2 according to the amount of Li inserted into or removed from the cathode. Several qualitative features are immediately evident. First, the spectra for KLi_xFeS_2 with $x = 0$ and $x = 1$ are relatively simple, being dominated by single quadrupole split doublets. Second, $KFeS_2$ appears to be the ultimate product upon recharge of the cell. And third, the changes evident during the first discharge of the cell are not just simply reversed by recharging the cell. A comparison of the spectra at $x = 0.5$, both on discharge and on recharge, is shown in Fig. 3.

As an aid in the quantitative interpretation of the results several spectra were modeled and the data fitted by the method of least squares. The spectrum of $KLi_{0.5}FeS_2$ (first discharge) was modeled as a sum of eight Lorentzian peaks. Three new Fe sites [Fe(1), Fe(2), and Fe(3)] in addition to the site in $KFeS_2$ contribute to the spectrum. Each iron site produces a quadrupole split doublet. In the fitting procedure each doublet was constrained to be symmetrical and the background was taken to be a constant function of

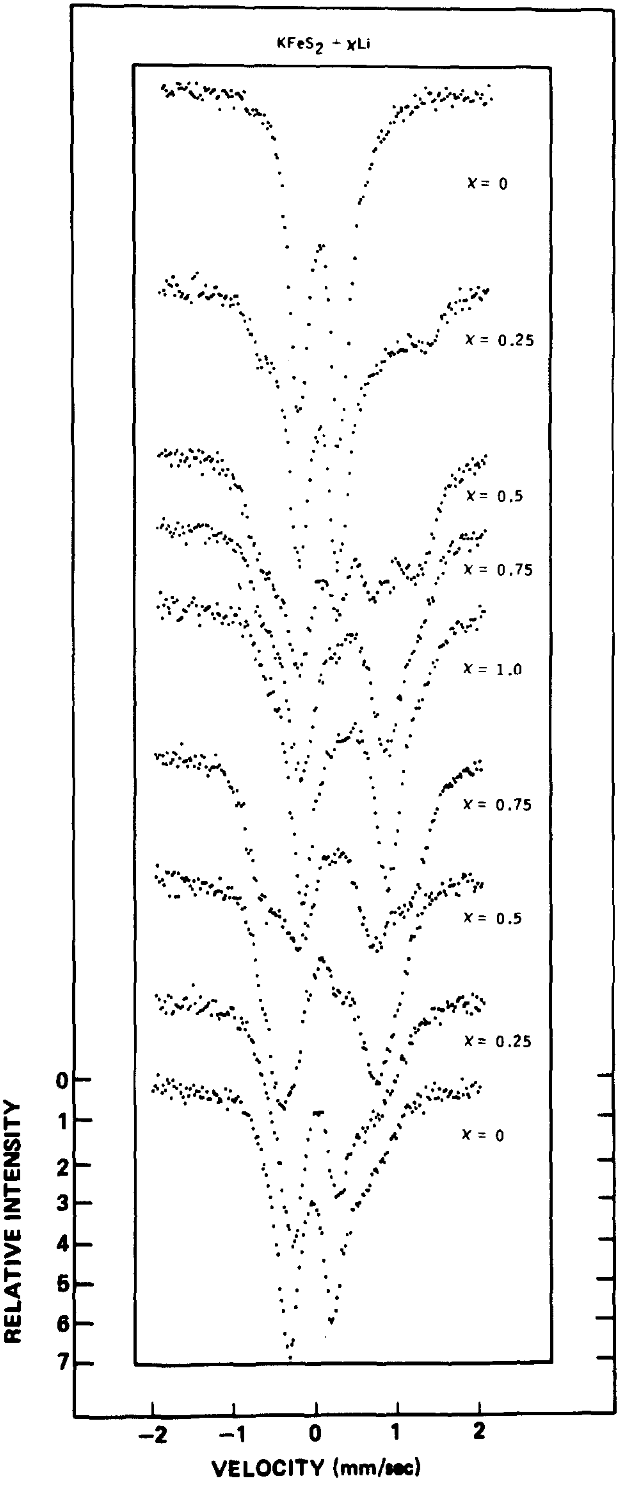

FIG. 2. Mössbauer data for KLi_xFeS_2 as a function of x.

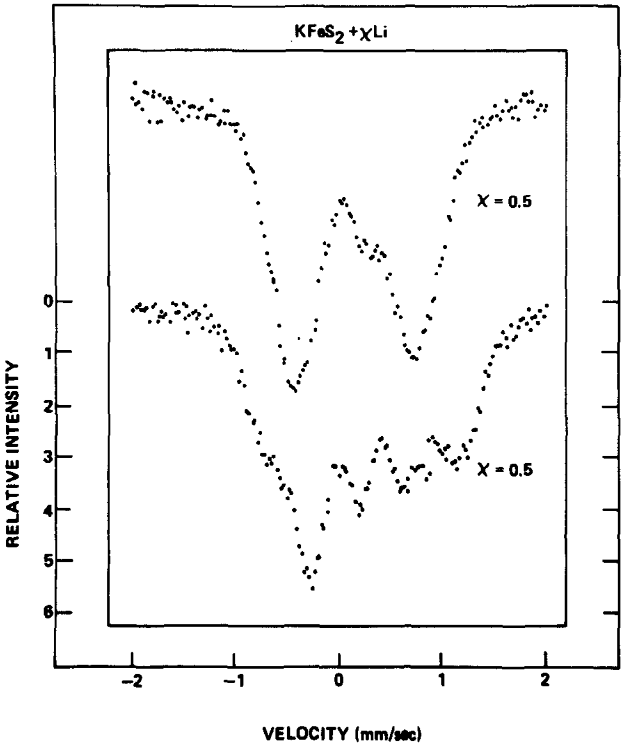

FIG. 3. Mössbauer data for $KLi_{0.5}FeS_2$. Top, recharge; bottom, discharge.

TABLE I

MÖSSBAUER RESULTS FOR $KFeS_2$/Li

		V	IS (mm/s)[a]	QS (mm/s)	%
$KLi_{0.5}FeS_2$ (discharge)	$Fe^{3+}(KFeS_2)$	2.95	0.22	0.46	20
	Fe(1)	2.65	0.34	0.95	26
	Fe(2)	2.35	0.46	1.88	37
	Fe(3)	1.95	0.62	0.85	17
$KLiFeS_2$	$Fe^{3+}(KFeS_2)$	2.95[b]	0.22[b]	0.46[b]	6
	Fe(1)	2.65[b]	0.34[b]	0.95[b]	1
	Fe(2)	2.35[b]	0.46[b]	1.88[b]	1
	Fe(3)	2.15	0.54	1.02	92
$KLi_{0.75}FeS_2$ (recharge)	$Fe^{3+}(KFeS_2)$	—	—	—	0
	Fe(1)	2.57	0.37	0.84	36
	Fe(2)	2.35	0.46	1.76	47
	Fe(3)	2.10	0.56	0.84	17

[a] Isomer shifts relative to iron.

[b] Constrained.

velocity. The final model consisted of 25 parameters of which 17 were taken as independent. The fit yielded a final reduced χ_ν^2 equal to 1.1. If the observed scatter of the data about the fitted spectrum is consistent with the experimental uncertainties in the data, the χ_ν^2 should ideally be 1.0. Final IS and QS values are tabulated in Table I and the resolved spectrum shown in Fig. 4.

A satisfactory fit for the $KLiFeS_2$ spectrum was obtained using a very simple model based on the results from $KLi_{0.5}FeS_2$. The spectrum is dominated by a single doublet but has minor contributions from three doublets of low intensity. The peak positions and widths for the three minor doublets were constrained to the values obtained from $KFeS_2$, Fe(1), and Fe(2) in the $KLi_{0.5}FeS_2$ spectrum. The peak positions and peak width for the major doublet were fitted as were the areas of all four symmetrical doublets as well as background parameter. Thus, of the 25 parameters in the model only 8 were adjusted, giving a $\chi_\nu^2 = 1.9$. The final isomer shifts (IS) and quadrupole splittings (QS) are tabulated in Table I. The isomer shift and quadrupole splitting of the major doublet are close to the values obtained for Fe(3) in $KLi_{0.5}FeS_2$. The peak positions in the two spectra differ only in the slight shift to lower energy of the low-velocity component of the major doublet.

Finally, the spectrum of $KLi_{0.75}FeS_2$ (first recharge) was fitted ($\chi_\nu^2 = 1.6$) to three symmetrical quadrupole doublets which corresponded to Fe(1), Fe(2), and Fe(3). The spectrum contained no evidence of any $KFeS_2$. Final IS and QS values are tabulated in Table I.

The remaining spectra can be seen, qualitatively, to evolve from or into the representative compositions which were fitted quantitatively. Consequently further detailed analysis was not considered necessary.

n-Butyl Lithium Reactions

$KLiFeS_2$ can be prepared by reaction of *n*-butyl lithium with $KFeS_2$. However, it is difficult to prevent the presence of unreacted $KFeS_2$ arising from further reduction of

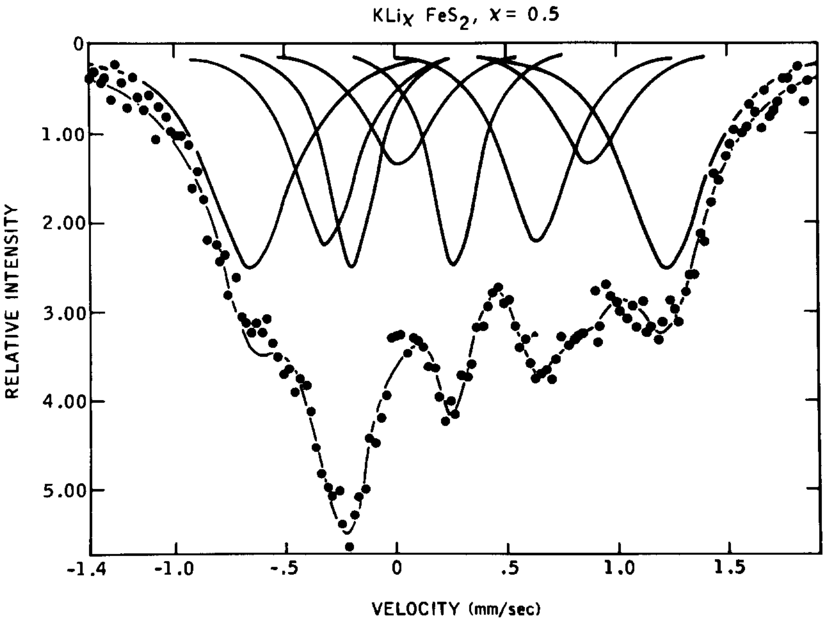

FIG. 4. Fitted Mössbauer spectrum for $KLi_{0.5}FeS_2$ (discharge).

$KLiFeS_2$ to iron metal. To overcome this problem, a sample of overall composition $KLiFeS_2$ prepared by reaction of $KFeS_2$ with a stoichiometric amount of *n*-butyl lithium was sealed under vacuum in a graphite-lined silica tube and annealed at 600°C for 25 days. The X-ray pattern of the resulting product was sharp and was indexed on a body-centered tetragonal unit cell with lattice parameters $a = 3.938(2)$ Å and $c = 13.135(5)$ Å. The observed and calculated *d* spacings are given in Table II. Chemical analysis for lithium and potassium gave a Li:K ratio of 1.0:1.01.

TABLE II

X-RAY DATA FOR $KLiFeS_2$ ANNEALED AT 650°C[a]

2θ	I/I_0	*d* (obs)	*d* (calcd)	*hkl*
13.52	44	6.55	6.57	002
27.14	14	3.285	3.284	004
30.50	100	2.931	2.928	103
32.14	16	2.785	2.785	110
35.02	67	2.562	2.564	112
41.29	12	2.186	2.189	006
			2.185	105
42.54	24	2.125	2.124	114
46.08	45	1.970	1.969	200
48.20	4	1.888	1.886	202
53.20	50	1.722	1.721	116
54.25	5	1.691	1.694	107
			1.689	204
55.93	9	1.644	1.642	008
56.25	23	1.635	1.634	213
63.50	4	1.465	1.464	206
67.15	7	1.394	1.392	220

[a] $a = 3.938(2)$ Å, $c = 13.135(5)$ Å.

Discussion

The Mössbauer spectra obtained on discharge for the compositions $x = 0.25$, 0.50, and 0.75 in $KLiFeS_2$ all contain the quadrupole split doublet characteristic of unreacted starting material, $KFeS_2$. However, at $x = 1.0$ the amount of $KFeS_2$ remaining is small (6%). That any $KFeS_2$ remains at this composition is likely to be a consequence of side reactions associated with the difficulty in titrating the cell to $KLiFeS_2$ above 1.3 V when no graphite has been added as a conducting diluent to the cathode. Under the experimental conditions, solvent decomposition at 1.3 V may have introduced a sufficiently large error in the coulometric titration to account for the residual amount of $KFeS_2$ observed when x was nominally 1.0. The further reduction of $KLiFeS_2$ to K_2S, Li_2S, and Fe is a possible alternative side reaction at low voltage. Since 2 moles of Li are required to produce 1 mole of Fe it is unlikely that the 3% iron metal necessary to account for the small amount of $KFeS_2$ would have been observed. For lower lithium contents the cell reaction occurs at higher voltages and such side reactions do not present a problem. Apart from the small amount of residual $KFeS_2$, the spectrum at $KLiFeS_2$ is a simple quadrupole split doublet; at intermediate compositions the spectra are more complex and indicate the presence of three distinct iron species apart from Fe^{3+} in $KFeS_2$. The Mössbauer data support the mechanism proposed for the initial reaction of lithium with $KFeS_2$:

$$KFeS_2 + xLi \xrightarrow{\text{fast}} xKLiFeS_2 + (1-x)KFeS_2, \tag{1}$$

$$xKLiFeS_2 + (1-x)KFeS_2 \xrightarrow{\text{slow}} KLi_xFeS_2. \tag{2}$$

On the time scale of the coulometric titration, the second reaction occurs to some extent and at intermediate compositions other iron sites in addition to those corresponding to $KFeS_2$ and $KLiFeS_2$ are observed. On the much faster time scale of a constant current discharge (typically 5–10 hr for a cell of similar capacity) only the first reaction occurs to a significant extent and consequently the voltage is nearly constant as a function of composition. The appearance of new iron sites at intermediate compositions is to be associated either with chemically distinct iron atoms in a continuous nonstoichiometric phase KLi_xFeS_2 or with the presence of distinct phases KLi_xFeS_2 with closely spaced compositions (see below).

On recharge of the cell, the Mössbauer spectrum shows that $KFeS_2$ is reformed. However, a small amount of another phase is present due to the small coulometric titration error introduced at the end of the discharge. The error may have been slightly increased at the end of recharge since the high upper voltage (2.60 V) may have resulted in some additional solute decomposition.

A comparison of the discharge and recharge spectra show some similarities and some important differences. $KFeS_2$ is not observed to be reformed until $x \leq 0.5$. The residual $KFeS_2$ observed in the spectrum at $x = 1.0$ is not observed in the recharge spectrum at $x = 0.75$ (see Table I) as a consequence of the slow equilibrium process represented by reaction (2). The same three inequivalent iron sites observed in the discharge spectra in addition to Fe^{3+} in $KFeS_2$ are again observed in the recharge data. The Mössbauer data then support a recharge mechanism:

$$KLiFeS_2 \rightarrow KLi_xFeS_2 + (1-x)Li, \quad (3)$$

where the lower bound on x lies between 0.5 and 0.25 and

$$KLi_xFeS_2 \rightarrow KFeS_2 + xLi. \quad (4)$$

Reaction (3) occurs with minimal structure change and KLi_xFeS_2 is either a continuous nonstoichiometric phase or a series of closely spaced ordered compositions. Insufficient data are available at present to distinguish between these two possibilities or to precisely define the lower bound on x. Reaction (4) is slow and does not occur to a significant extent in constant current cycling.

The Mössbauer data generally confirm the conclusions based on the electrochemical data. However, because the Mössbauer data are sensitive to the iron environment additional information may be obtained concerning the structural changes which occur. Such an analysis is aided in this particular case by the availability of Mössbauer data for a number of closely related systems containing iron which is tetrahedrally coordinated by sulfur and in which the iron occurs in +2, +3, and intermediate oxidation states (see Table III). Examination of these data suggests that for Fe–S compounds (i) an isomer shift of 0.17–0.20 mm/sec with an associated quadrupole splitting of 0.4–0.6 mm/sec is diagnostic for high-spin tetrahedral Fe^{3+}, (ii) an isomer shift of 0.6 mm/sec with a large quadrupole splitting is indicative of high-spin tetrahedral Fe^{2+}, and (iii) mixed valence tetrahedral Fe–S systems have intermediate isomer shifts. Hoggins and Steinfink (*10*) summarized the available data for the alkali and alkaline earth metal iron sulfides and some data for other sulfides containing tetrahedrally coordinated iron by means of an empirical relation between the isomer shift (IS) and the mean iron oxidation state (V):

$$IS = 1.4\text{–}0.4\ V\ (\text{mm/sec}).$$

From a comparison of the isomer shift of the major component at the end of the discharge ($x = 1.0$, Table I) with the data in Table III, it is likely that the divalent iron atoms in $KLiFe(II)S_2$ are tetrahedrally coordinated by sulfur. In $KFeS_2$, itself, K^+ irons occupy distorted cubic antiprismatic sites and the FeS_4 tetrahedra form infinite chains by edge sharing (Fig. 1). We also note large alkali metal ions have a strong preference for eight coordinate sites in ternary sulfides where the other metal is tetrahedrally coordinated. Two simple structural possibilities for the arrangement of the $Fe(II)S_4$ tetrahedra in $KLiFeS_2$ into a framework with the correct FeS_2 composition are: (i) non-crosslinked edge-shared chains as in $KFeS_2$ or (ii) a plane net in which each tetrahedron shares all four corners as found in $TlFeS_2$ (*11*). Each of

TABLE III

MÖSSBAUER PARAMETERS AT ROOM TEMPERATURE FOR THE ALKALI AND ALKALINE EARTH IRON SULFIDES

Compound	Oxidation state	IS (mm/sec)	QS (mm/sec)	Ref.
"$NaFeS_2$"	3	0.36	0.58	(*13*)
$KFeS_2$	3	0.19	0.53	(*14*, *15*)
$RbFeS_2$	3	0.19	0.45	(*13*)
$CsFeS_2$	3	0.18	0.46	(*13*)
$Ba_9(Fe_2S_4)_8$	2.88	0.20	0.65	(*16*)
Ba_2FeS_3	2	0.62	2.56	(*16*)
$BaFe_2S_3$	2	0.41	0.60	(*16*)
$Ba_7Fe_6S_{14}$	2.33	0.17	1.13	(*16*)
		0.39	1.46	
		0.66	1.33	
Ba_6FeS_{15}	2.25	0.47	0.68	(*16*)
$Ba_{15}Fe_7S_{25}$	2.85	0.20	0.91	(*17*)
Ba_3FeS_5	4	0.17	0.50	(*17*)
$Ba_4Fe_2S_6[S_{2/3}(S_2)_{1/3}]$	3	0.20	0.45	(*18*)
		0.20	0.90	

these frameworks contains an additional set of tetrahedral sites related by a translation from those occupied by Fe. The small Li^+ cation could be accommodated into either network by filling some or all of this second set of sites to give a composition $K(LiFe)S_2$. Li^+ in sulfur lattices tends to adopt tetrahedral coordination and is not averse to edge sharing, e.g., in Li_2S.

The sample of $KLiFeS_2$ annealed at high temperature was indexed as a body-centered tetragonal phase with lattice parameters $a = 3.938$ Å, $c = 13.135$ Å. A comparison of these lattice parameters with the lattice parameters of $TlFeS_2$ and with the tetragonal subcell parameters of $M_2M_3'S_4$ (M = Rb, Cs, and M' = Co, Mn) [(*12*); Table IV] suggests a similar structure for $KLiFeS_2$ with K^+ ions in cubic sites between layers of tetrahedra containing Li^+ and Fe^{2+}. A complete determination of the structure of $KLiFeS_2$ is in progress. It is interesting to note that the existence of the compounds $M_2M_3'S_4$ suggests that complete tetrahedral site occupancy is not necessary for stability of this type of layer structure when M is a large alkali metal.

At intermediate compositions the Mössbauer spectra indicate two kinds of iron atom with isomer shifts of 0.34–0.37 and 0.46, respectively, in both the discharge and recharge reactions. These shifts are intermediate between those expected for tetrahedral high-spin Fe(III) and high-spin Fe(II). Thus, the Hoggins and Steinfink empirical correlation between the isomer shift and iron

TABLE IV

LATTICE PARAMETERS (Å) OF CuTe-RELATED METAL SULFIDES

	a	*b*	*c*
$TlFeS_2$	3.753	—	13.342
$Rb_2Mn_3S_4$	5.845 (4.13)[a]	11.21 (3.96)	13.66
$Cs_2Mn_3S_4$	5.92 (4.18)	11.47 (4.05)	14.16
$Rb_2Co_3S_4$	5.64 (3.99)	11.04 (3.90)	13.37
$Cs_2Co_3S_4$	5.73 (4.04)	11.23 (3.97)	13.88
$KLiFeS_2$	3.938	—	13.135

[a] Numbers in parentheses are the tetragonal subcell parameters.

oxidation state can be used to calculate the oxidation state (V) of each of the four types of iron atoms evident from the spectrum of $KLi_{0.5}FeS_2$ formed on discharge (see Table III). The relative intensities of the four quadrupole split doublets can then be used to calculate an average oxidation state of 2.48, in excellent agreement with the 2.50 value from the coulometric titration. A similar analysis of the spectra obtained for $KLiFeS_2$ and $KLi_{0.75}FeS_2$ formed on recharge leads to results where the agreement is not nearly so good (2.15 compared with 2.0 and 2.39 compared with 2.25). However, at these compositions there is a small error in the coulometric titration as discussed above. Furthermore, the resolutions in these spectra are much poorer than the resolution in the $KLi_{0.5}FeS_2$ spectrum. In order not to overparameterize the model, we chose to increase the number of constraints. In particular, the velocity parameters of the peaks corresponding to the minor components in the $KLiFeS_2$ spectrum were constrained to the values determined for the $KLi_{0.5}FeS_2$ spectrum. This obviously introduces an additional error in the result obtained from the isomer shift/oxidation state correlation. Finally, it must be recognized that the empirical correlation itself was derived from data which exhibited a range of isomer shift values for a particular oxidation state. Thus, it is probably unreasonable to expect agreement to be better than 5% to 10%. An explanation of the structural origin of the two iron sites observed at intermediate compositions requires additional data.

Conclusions

The results discussed above demonstrate that Mössbauer spectroscopy can be successfully used to obtain information about the chemical reactions and structural changes which occur on discharge and recharge of lithium at iron containing cathodes. The data obtained for $KFeS_2/Li$ in conjunction with X-ray diffraction and electrochemical measurements have led to a good understanding of the reaction of $KFeS_2$ with lithium. Some problems, however, remain to be solved. In particular, the structure of the phase KLi_xFeS_2 has not yet been determined in detail and it is not certain whether the compound has a wide nonstoichiometric range or if there are a series of ordered intermediate phases. The synthesis of $KLiFeS_2$ has been successfully carried out at high temperature and it has been recently shown (*19*) that iodine oxidation is an effective route to intermediate compositions. These results and further work aimed at resolving the remaining questions will be the subject of a future report.

Acknowledgments

We are grateful to J. C. Scanlon for the construction of the Mössbauer cell, and S. M. Rich and J. A. Panella for sample preparation and cathode fabrication.

References

1. A. J. JACOBSON, M. S. WHITTINGHAM, AND S. M. RICH, *J. Electrochem. Soc.* **126**, June 1979.

2. P. PALVADEAU, L. COIC, J. ROUXEL, AND J. PORTIER, *Mater. Res. Bull.* **13**, 221 (1978).

3. M. S. WHITTINGHAM, *Progr. Solid State Chem.* **12**, 41 (1978).

4. M. EISENBERG AND M. WILLIS, *in* "Electrochemical Society Abstracts," p. 38, Atlanta (1977).

5. A. H. THOMPSON AND M. S. WHITTINGHAM, *Mater. Res. Bull.* **12**, 741 (1977).

6. A. LÉMEHAUTÉ, G. OUVRARD, R. BREC, AND J. ROUXEL, *Mater. Res. Bull.* **12**, 1191 (1977).

7. F. J. DISALVO, M. EIBSCHUTZ, D. W. MURPHY, AND J. WASZCZAK, *Bull. Amer. Phys. Soc.* **23**, 244 (1978).

8. R. R. CHIANELLI, B. M. L. RAO, AND J. C. SCANLON, *J. Electrochem. Soc.* **125**, 1563 (1978).

9. "Inorganic Syntheses" (E. G. Rochow, Ed.), Vol. 6, McGraw-Hill, New York (1960).

10. J. T. HOGGINS AND H. STEINFINK, *Inorganic Chem.* **15**, 1682 (1976).

11. A. KUTOGLU, *Naturwissenschaften* **61**, 125 (1974).
12. W. BRONGER AND P. BOTTCHER, *Z. Anorg. Allg. Chem.* **390**, 1 (1972).
13. W. KERLER, W. NEUWIRTH, E. FLUCK, P. KUHN, AND P. ZIMMERMAN, *Z. Physik.* **173**, 321 (1963).
14. C. A. TAFT, D. RAJ, AND J. DANON, *J. Phys. Chem. Solids* **36**, 283 (1975).
15. D. RAJ AND S. P. PURI, *J. Chem. Phys.* **50**, 3184 (1969).
16. W. M. REIFF, I. E. GREY, A. FAN, Z. ELIEZER, AND H. STEINFINK, *J. Solid State Chem.* **13**, 32 (1975).
17. J. T. LEMLEY, J. M. JENKS, J. T. HOGGINS, Z. ELIEZER, AND H. STEINFINK, *J. Solid State Chem.* **16**, 117 (1976).
18. J. T. HOGGINS, L. E. RENDON-DIAZMIRON, AND H. STEINFINK, *J. Solid State Chem.* **21**, 79 (1977).
19. A. J. JACOBSON AND S. M. RICH, to be published.